SUMMARY REPORT

Project: PN-III-P4-ID-PCE-2016-0833

Period covered: July 2017 – Sept. 2018

Introduction:

There is an ever-growing demand for data storage capacities in basically all technology and societal fields, with the advent of new concepts such as Data Centers, Cloud Computing and Internet-of-Things that shows steady growth of about 40% per year. Magnetic storage has shown tremendous development in area density and speed, over the last 50 years, however the current hard disk storage is a mature, quite limited, technology with only incremental enhancements possible. As such, a radically new technology will soon be required to keep up with the demand. There are two major breakthroughs that have the potential to allow improvement of the read-write process (speed and power). The first one is represented by our results, obtained in the frame of this project [1], where we have investigated nanomagnet-logic structures compatible with MTJ elements, made of FePt/Cu/Fe trilayers. By investigating the remanent coupling between the hard and soft magnetic layers, through the non-magnetic spacer layer of Cu, we have shown with good precision, how this coupling angle can be conveniently adjusted with high degree of remanence by shortly applied external magnetic fields, via a mechanism called the interlayer exchange coupling. Considering thus this coupling angle as the information storage vector, we propose that not only two magnetization directions can be stored in a magnetic unit cell (up and down) but several orientations of the magnetization vector, orientations given by the appropriately tuned remanent coupling angle, may be stored and retrieved. We are proposing thus an alternative solution to encode information in magnetic films that goes beyond the conventional way of digital magnetic recording. Extremely important for future applications of this concept, we demonstrate, that the remanent coupling angles can be read out via magneto-optical or magneto-resistance effects. In principle, this approach allows to design novel memory cells for advance data storage devices, where multiple states per unit cell can be generated and recorded.
The second breakthrough is represented by the recently reported magnetization reversal by femtosecond laser pulses in thin ferromagnetic Gd/Fe/Co films as well as in many other magnetic materials including rare-earth free transition metal multilayers such as Mn-Fe-Al and Co/Ir and CoNiPt/Ir based heterostructures [S. Mangin et al. Nature Materials 13 (2014) 286–292]. Conceptually it represents a new way to control the magnetic state of a medium, at the highest efficiency and shortest possible time-scale. Magnetization reversal by optical means can be done using the laser in the femtosecond regime. The femtosecond magnetic switching has the capacity of pushing the limit of data transfer rates to terabit-per-second range in magnetic recording, at femtojoule per bit switch energies [T. Li et al. Nature 496 (2013) 69–73]. However, there is still long way to go from the fundamental science to scaling up the technology and there is need for taking steps in order to close the gap towards industrially relevant applications.

Project objectives:

1) the creation of magnetic tunnel junction (MTJ) made of rare earth free magnetic compounds (based on Mn/Ir, Mn/Fe/Pt or Co/Ir) as the base foundation for memories; 2) the demonstration of magnetization reversal by femtosecond laser pulses in the MTJ stack; 3) the validation of the performances by testing of the element of memory demonstrator; 4) the conception of an integration platform made of array of MTJs optically switched.

Scientific results:

Stage 1: Creation of a MTJ multilayer as a basis for memory elements

In its simplest form, a MTJ is a trilayer sandwich consisting of two ferromagnetic layers separated by a ultrathin non-magnetic barrier layer. If a voltage is applied to the top and bottom of this structure, and the barrier layer is sufficiently thin, electrons can flow by quantum tunneling through the barrier layer. For tunneling between two magnetic layers the tunneling current is maximum if the magnetization directions of the two magnetic layers are parallel and minimum if their magnetizations are oriented antiparallel. The phenomenon is called tunneling magneto-resistance and is a consequence of the spin dependent tunneling along (CIP) or across (CPP) the structure. The first step that we undertook in the 1st stage of the project, for the creation of the MTJ multilayer, consisted of the development of a trilayer structure made of polycrystalline Fe(10 nm)/Cu(0.6…6.4 nm)/FePt(30 nm) nanolayers that have been prepared by high vacuum ($p = 3 \cdot 10^{-7}$ mbar) rf-magnetron sputtering in an Ar atmosphere of $p = 1 \cdot 10^{-2}$ mbar. These layer systems were deposited on amorphous Ta seed layer on super polished Si substrates and on top they were finally coated against oxidation by 3 nm of Ta_2O_5. To investigate the coupling and conduction phenomena, depending on the tunable thickness of the non-magnetic layer, the sample has been constructed in such a way as to achieve a continuous variation of the Cu layer thickness along the structure. For this purpose, a wedge-shaped Cu spacer layer (slope: S_{max} = 3.3 nm/cm) has been synthesized. The $Fe_{50}Pt_{50}$ layer achieved its $L1_0$-phase structure and became magnetically hard after high vacuum annealing at T = 800 K for t = 15 min. The polycrystalline character of the FePt was determined via atomic force microscopy and x-ray diffraction measurements. We obtained an in-plane texture of the tetragonal c-axes of the grains with an average grain size of about L = 20 nm. The random distribution of the grains c-axes results in no preferred direction of the in-plane magneto-crystalline anisotropy after deposition. Surface quality has been checked by x-ray reflection in grazing incidence geometry, data from which a root-mean-square roughness of about σ = 0.4 nm for the top magnetic layer has obtained. The surface roughness of all interfaces of the system did not exceed σ = 0.7 nm.

   The magnetic properties of the layer system were characterised by longitudinal MOKE measurements at room temperature. Hysteresis loops of the coupled layer system indicate that the magnetic layers are ferromagnetically coupled over the whole range of Cu thickness because only negative exchange fields were observed.
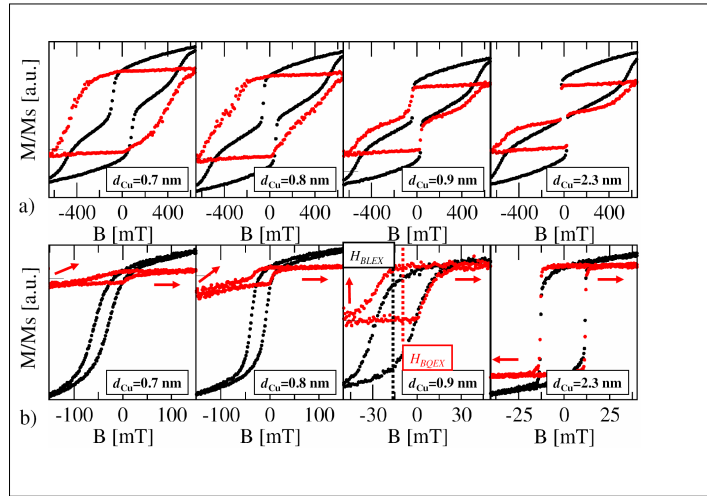
Fig.1. Room temperature MOKE hysteresis loops for different Cu interlayer thicknesses. The black curves are typical loops - measured with applied fields - the red curves are measurements in remanence mode, where the magnetic fields were temporarily applied for $t = 1$ s. a) major loops and b) easy-axis minor loops, where only the magnetisation direction of the soft magnetic layer is rotating. Additionally, the definition of the bilinear and biquadratic exchange fields (H_{BLEX}, H_{BQEX}) is demonstrated.

In fig. 1 are displayed some examples of the hysteresis loops for different Cu interlayer thicknesses, in particular major (Fig. 2a) and minor (Fig. 2b) loops (B parallel to the FePt easy axis). The black curves are describing typical loops - measured with continuously applied fields – while the red curves are special measurements in remanence mode, where the magnetic fields were temporarily applied for a finite time period $t = 1$ s. In this manner each point of the hysteresis loops was measured in remanence mode. One can see, that for a Cu thickness of about $d_{Cu} = 2.3$ nm the magnetisation of the Fe layer is almost freely adjustable, because the exchange field is negligibly low. For Cu thicknesses less than $d_{Cu} = 2.3$ nm, bi-quadratic coupling is induced and thus different coupling angles are obtained, depending on the magnetic field magnitude and the thickness of Cu. This behaviour is displayed in fig. 2b) with the help of the red arrows inside the minor loop graphics that show the Fe layer magnetisation direction. These different coupling angles may be detected and can be an alternative solution to encode information in magnetic films, in scenarios where multiple states per unit cell (not only "up" and "down") can be generated and recorded. Such result in spin manipulation and magnetization detection that refers to the observation of the interlayer exchange coupling (IEC) in trilayer systems made of hard and soft magnetic layers, with a metallic non-magnetic layer in between, can be foundational for future applications. We have demonstrated that depending on the layer thickness, the orientation of the magnetic layers can be tuned to either antiparallel or parallel, as required in the MTJ stack. We have also shown that by tuning the IEC we can orient the spin and detect its orientation not only in up and down position, but also in intermediate positions and this opens pathways towards recording multiple bits of information onto the same stack.

The layer stack of the MTJ elements have been determined based on the specific needs of the function to be performed. The systems chosen for the MTJ stack components are derived from Mn-Al and Ir-Mn. Such samples have been deposited by DC – RF sputtering in our dedicated facility at NIMP, a UHV chamber (10^{-8} mbar) with possibility

of simultaneous sputter from 3 targets. Rigorous control of stoichiometry and evaporation rate can be achieved during fabrication. During deposition the base pressure was 3×10^{-6} mbar, used for degassing the samples for 2 hours. The layers were obtained in Ar plasma of low pressure. By applying the rf field the Ar ions are accelerated towards an electrode that contains the metallic target. Ar ions sputter metallic atoms from the target that afterwards are deposed onto the substrate fixed on top of the other electrode (10 cm between electrodes). The working power was ranging between 40 and 180 W, depending on the nature of the metal sputtered. Layered systems with compositions such as [Mn-Ir]/57Fe/Cu/Si and [Mn-Ir]/57Fe/FeNiCr/Si have been prepared and characterized.

In order to better quantify the Mn influence on the magnetic and switching behavior of the free magnetic layer in the MTJ stack, several other Mn containing systems have been prepared. A particularly favorable case is represented by the compound $Mn_{55}Al_{45}$ suitable for inclusion in the MTJ stack. For this compound, a structural phase transition has been documented and monitored [A.D. Crisan et al. Mater Charact. 140 (2018) 1-8] during the present project. The ε to β-Mn phase transition is particularly favorable for inducing magnetic anisotropy in the case of layer compounds in the MTJ stack. The temperature evolution of the phase composition in the $Mn_{55}Al_{45}$ sample has been followed by using structural temperature-dependent XRD measurements using synchrotron radiation. All the recorded diffractograms were analyzed by a whole-profile fitting procedure in order to retrieve the structural parameters (lattice parameters, relative phase abundance, grain size). As mentioned before, at room temperature, the synchrotron diffractogram of the *as-cast* $Mn_{55}Al_{45}$ alloy have shown mainly a mixture of γ_2 (Al_8Mn_5) (around 75%) and ε-phase (around 25%). The ε to β-Mn phase transition is initiated at approx. 470°C. The amount of ε phase gradually decreases and the ε phase disappears above 520°C. The diffraction peaks of the β-Mn phase become visible above this temperature, and the amount of β-Mn increases to reach about 25% at 700°C the maximum temperature attained in this study. The amount of the γ_2 (Al_8Mn_5) phase is constant throughout the *in-situ* temperature-resolved diffraction experiment, although its relative fraction changes, due to the variation of the total scattered X-ray intensity caused by the decomposition of the ε phase and the subsequent formation of the β-Mn phase. After constant-rate heating to 700°C, followed by isothermal treatment at this temperature for about 20 min and cooling down to ambient temperature, the specimen consists of a mixture of 75% γ_2 (Al_8Mn_5) phase and β-Mn phase, respectively (Fig. 2).
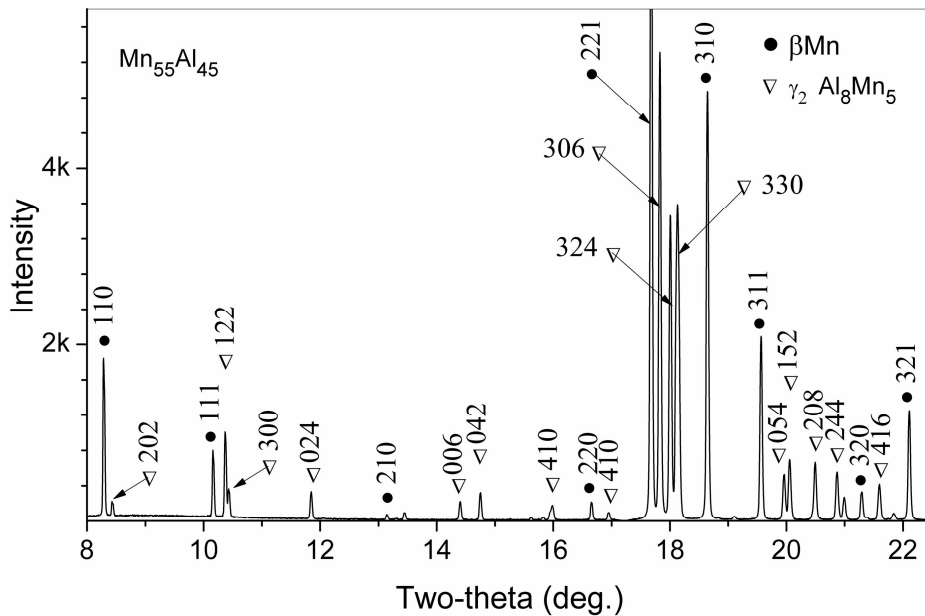
Fig. 2 Indexing of the room temperature XRD pattern of $Mn_{55}Al_{45}$ after heating, isothermal treatment and subsequent cooling.
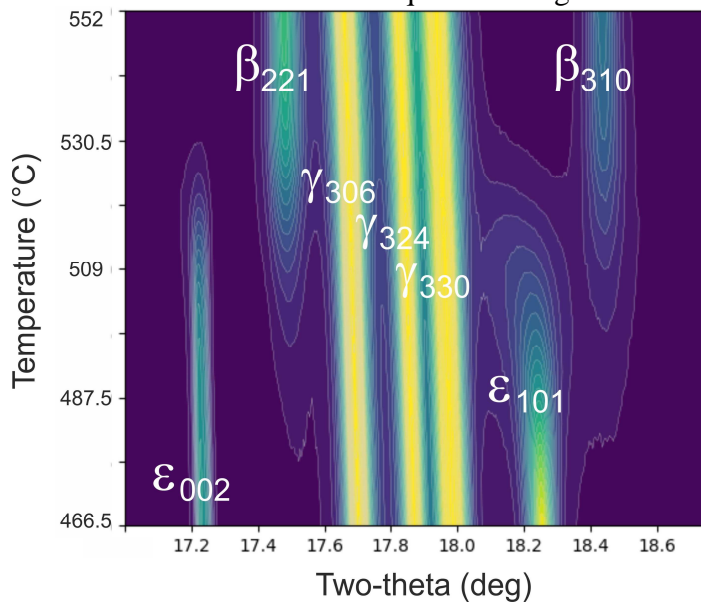
Fig. 3 Contour plot of the diffracted X-ray intensity for the ε to β-Mn phase tranformation during heating.

Figure 3 shows the diffracted X-ray intensity recorded from X-ray spectra at various temperatures in the range of the ε to β-Mn phase transformation (466°C to 552°C). It can be observed that the phase transformation occurs abruptly, within a 20°C temperature range, however there is a small temperature range of about 5 °C, centered at around 510-515°C where the two phases co-exist. The lines of the majority γ_2 phase have almost the same intensity throughout the whole investigated temperature range.

In conclusion, with respect to the 1st stage all the activities proposed in the work plane have been undertaken and the objectives have been attained. The results of the 1st stage, a stage that has been concluded in December 2017, have been categorized in agreement to the project objectives to be fulfilled in scientific, project management and dissemination. Scientific results, linked to and derived from the 1st stage activity related to the creation of MTJ elements, were mainly represented by the design of the free layer of the MTJ stack, the design of the MTJ multilayer structure. Project management results included the creation of the website, the risk management and the quality assurance plans as well as the annual report plan. The dissemination results have been concluded with communications at international conferences and 1 publication in ISI ranked journal.

Stage 2: Demonstration of light assisted magnetization reversal of the MTJ element. Conceptualization of the magneto-optic technology for integration onto Si substrate. (dec. 2018).

During the 2nd stage of the project, during 2018, the activities proposed in the work plan are related to development of MTJ elements for photonic assisted magnetization reversal and the realization of a magnetization switching of the free layer in MTJ with the help of a pulsed laser (photonic assisted switching mechanism). For this purpose, a MTJ structure made of multilayered heterostructures of Ta/ GdFeCo/Cu/[Pt-Co]/Ta have been prepared. The depositions have been made by rf and dc sputtering using the dedicated UHV sputtering facility described above. Rigorous control of the sputtering rates made possible the realization of the layered structure without significant intermixing of the sputtered elements, as proven by In situ observations and X-ray reflectivity studies.

It has been recently proven by [R. John et al. Scientific Reports 7 (2017) 4114] that also FePt nanoparticles may exhibit magnetization reversal by femtosecond laser pulses, and also the reversal occurs through two different mechanisms: the helicity-dependent all-optical switching where the reversed magnetic orientation is defined by the optical angular momentum (or the helicity of the circularly polarized laser light), and thermally driven switching caused by laser heating with linearly polarized light. The second mechanism occurs mainly in the rare earth ferromagnetic compounds and has been explained through parallel alignment of the rare-earth and transition-metal sublattice magnetisations below the picosecond timescale. For this reason, layered systems containing both FePt or CoPt hard magnet layers and RE – containing layers such as GdFeCo are of interest for realization of our MTJ elements. Considering these issues, the choice of our heterostructure appears justified. The sample layout we prepared has the following deposition sequence: Glass substrate/Ta (3 nm)/[Pt(0.8 nm)/Co(0.7 nm)]5/Cu(8.1 nm)/Gd20(FeCo)80(5.6 nm)/Ta (3 nm). The individual GdFeCo and [Pt-Co] layers exhibit interlayer exchange coupling through the non-magnetic Cu layer, as obtained during the stage I of the project. The scheme of the layout model is provided in the Figure below. After performing the irradiation of the layout heterostructure with a 50 fs laser pulse we have measured the hysteresis loops and compared them with the ones measured before irradiations. The magnetic field has been applied perpendicular to the film surface. The magneto-optic Kerr effect usually measures the angle made by the K

vector (defined as the Kerr amplitude generated as a result of interaction of the light beam with the magnetization vector) with the normal plane of the film θ_K. The Kerr signal θ_K obtained for the MTJ heterostructure is presented in Figure 4. Normalized magneto-optic Kerr signal θ_K has been recorded as a function of the magnetic field that has been applied normal to the MTJ heterostructure plane. At very small negative fields we have recorded also minor loops (red and blue curves). These loops are showing no exchange bias behavior being centered on the x = 0 axis. These minor loops show sharp decrease of the magnetization from one spin state to another and accounts for the magnetization reversal of the free layer in the MTJ structure.
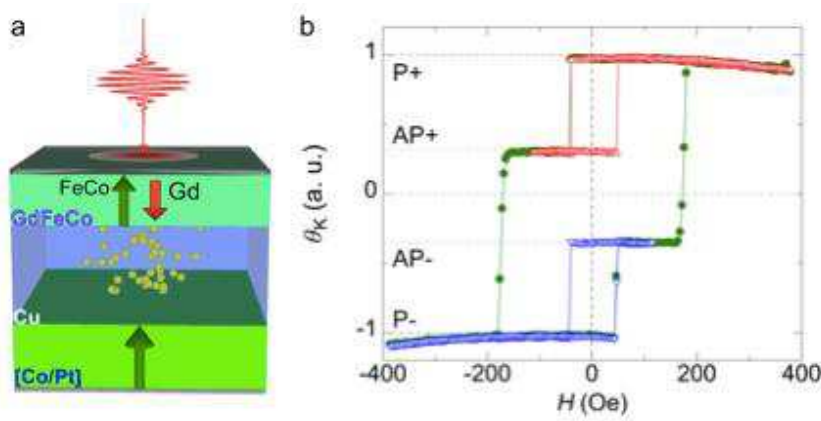
Fig. 4: Schematics of the MTJ structure made of Ta/ GdFeCo/Cu/[Pt-Co]/Ta. a) Sample layout of the model MTJ made of: Glass substrate/Ta (3 nm)/[Pt(0.8 nm)/Co(0.7 nm)]5/Cu(8.1 nm)/Gd20(FeCo)80(5.6 nm)/Ta (3 nm). The individual GdFeCo and [Pt-Co] layers exhibit interlayer exchange coupling through the non-magnetic Cu layer. Following laser irradiation on the GdFeCo side, high energy electrons are emitted by the surface of the free ferromagnetic layer, thus producing the magnetization switching of the [Co/Pt] magnetic layer. b) Kerr signal θ_K plotted as a function of the magnetic field (H) applied perpendicular to the film plane (minor loops proving the magnetization switching are shown in blue and red color).

The observed magnetization reversal mechanism is due to the electron flux determined by the irradiation with the laser pulse of the surface of the free ferromagnetic layer. These electrons hit the surface of the second ferromagnetic, hard magnetic, CoPt layer causing magnetization reversal in that layer. Magnetization vector of the two ferromagnetic layers may be reversed either parallel or antiparallel. The Kerr signal distinguishes clearly between four possible spin orientations. From the minor loops we estimated the magnetic exchange fields H_{BLEX} originating from the bilinear (ferromagnetic) coupling between the layers, as a function of interlayer distance. Two different coupling mechanisms excite the bilinear magnetic exchange fields: a magnetostatic interaction (so-called Nèel or orange-peel coupling), with an exponential decay and a RKKY coupling (also known as quantum well coupling) where the decay is quadratic and oscillating as function of the interlayer thickness d_{Cu}:

$$H_{Ex}(d_{Cu}) = (H_0/d_{Cu}{}^2)\sin(\phi + 2\pi d_{Cu}/\lambda) + H_s e^{-d_{Cu}/t_s} \quad (1)$$

Here the first term is describing the RKKY coupling field and the second term the magnetostatic (or dipolar) coupling field. The constants H_0, φ, λ corresponds respectively to the maximum exchange field, the phase shift and the oscillation period of the RKKY coupling and the constants H_s and t_s are respectively the dipolar field of the magnetostatic interaction and the thickness of the soft layer. Using equation (1) we fitted the bilinear exchange fields as function on the interlayer thickness. The results are displayed in fig. 5a and the estimated fit parameters are shown in Table 1.
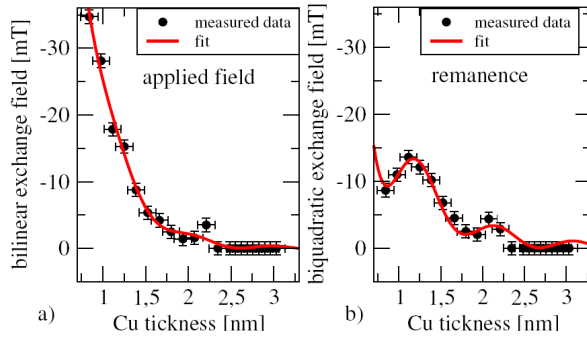
Fig. 4: Magnetic exchange fields as a function of interlayer thickness estimated from MOKE measurements with applied fields a) and in remanence mode b).

Parameter	H_{BLEX}	H_{BQEX}
H_0 [mT nm²]	-2.2	-6.0
Φ	-0.4	-1.0
λ [nm]	0.91	0.91
H_d [mT]	-347	-69.5
T [nm^{-1}]	0.37	0.61

Table 1: Calculated parameters as resulted from the fits using equation (1) with data shown in Fig. 5

We have also measured easy-axis minor loops in remanence mode, after temporarily applied magnetic fields. The areas of these minor loops are describing the biquadratic coupling energy $E_{BQ} = -J_2(m_1 \cdot m_2)^2$. However, the definition of the bilinear and biquadratic exchange fields is quite different, because of their asymmetric evolution. After the remanent coupling angles are induced to a maximum, only opposite applied fields are able to rotate the magnetisation vector back to a ferromagnetic alignment. There is no intrinsic reset force due to the biquadratic coupling. Nevertheless we used the definition for the bilinear exchange fields to estimate biquadratic exchange fields H_{BQEX} as function of the interlayer thickness, see Fig. 5b. We fitted these data using the same equation (1), the results of this fit being shown in Fig. 5. The parameters obtained from the fit are displayed in Table 1. One can see, that the influence of the oscillatory RKKY-coupling is more pronounced for the biquadratic exchange field than for the bilinear exchange field. Vlasko-Vlasov et al. have shown, that the field induced biquadratic coupling of a hard and soft magnetic layer can be described by an adaptation of the fluctuation model developed by Slonczewski. The assumption of this model is that the spatial coupling fluctuations are not caused by thickness variations of the nonmagnetic layer but by the spatial fluctuations of micromagnetic orientations of the hard magnetic layer. This leads to the same

biquadratic coupling behaviour as proposed in the model of Slonczewski. In this model, the magnitude of the BQ J_2 depends on the BL RKKY coupling J_1, the size of the micromagnetic orientation (grain size) L, the intralayer exchange stiffness A_s and the layer thickness D.

$$J_2 = 4 \frac{(J_1)^2 L}{\pi^3 A_s} \coth\left(\pi \frac{D}{L}\right) \qquad\qquad (2)$$

The remanent coupling angle between the magnetisation vectors can be calculated using the following formula: $\cos\theta_{rem} = (1-2f)J_1/2[N(f)J_2 - K_s]$, where the function $N(f)$ is depending on the external fields and accounts, in first order, for the number of rotated micro magnetisations and thus changing effectively the coupling constants J_1 and J_2. This mechanism results in a maximum of induced coupling angles, when the BL coupling constant J_1 is maximal.

In conclusion, the objectives foreseen for the 2nd year of the project development have been fully attained. Scientific results include the creation of MTJ elements for light assisted magnetization switching and the architectural design of the MTJ arrays with optical and electrical control. Due to the high potential of patenting our results, only a brief summary of our results may be publicly made available on the project webpage.